

Powered oscillator using ignitron switches

P. D. Nonn, A. P. Blair, K. J. McCollam, J. S. Sarff, and D. R. Stone

Citation: *Rev. Sci. Instrum.* **82**, 064701 (2011); doi: 10.1063/1.3589266

View online: <http://dx.doi.org/10.1063/1.3589266>

View Table of Contents: <http://rsi.aip.org/resource/1/RSINAK/v82/i6>

Published by the [American Institute of Physics](#).

Additional information on *Rev. Sci. Instrum.*

Journal Homepage: <http://rsi.aip.org>

Journal Information: http://rsi.aip.org/about/about_the_journal

Top downloads: http://rsi.aip.org/features/most_downloaded

Information for Authors: <http://rsi.aip.org/authors>

ADVERTISEMENT

physicstoday

Comment on any
Physics Today article.

Physics Today / Volume 63 / Issue 7 / July 2012
Previous Article | Next Article

Measured energy in Japan
David von Seggern
(dovseg@seismo.unr.edu) University of Nevada
July 2012, page 10
DIGITAL OBJECT IDENTIFIER
<http://dx.doi.org/10.1063/PT.3.1619>

The article by Thorne Lay and Hiroo Kanamori (2011) is an excellent review of the energy released by the 2011 Tohoku earthquake. While that of a 100-megaton explosion is approximately five times as much energy as that of a 20-megaton nuclear detonation event—a 40-megaton atmospheric event is approximately five times as much energy as that of a 10-megaton nuclear device. I believe the authors used the relation for seismic energy release rather than total strain energy release. The seismic energy underestimates the total strain energy release by a variable that depends on the fault plane. Accounting for total strain energy release would increase the earthquake energy number by orders of magnitude.

Despite the catastrophic damage potential of nuclear bombs, the forces of nature occasionally unleash much larger energy releases. Although the nuclear bombs are under our control, earthquakes, volcanic eruptions, and extreme weather events are not. However, by judicious preparation and avoidance measures, humans can significantly diminish the damage of natural events.

This article does not have any references.

Comment on this article
By the act of hitting a ball with a bat, one calculates the force energy to deliver the ball to its new location, but one must also take into account that the ball extended its energy release to that which became struck by the ball as its momentum ceased and passed energy to the struck team. Therefore the parameters of the damage extend into the future when the received energy to that pushed upon, later becomes released in a new event. Perhaps calculations of one added that in while another's calculations did not. E.M.C.
Written by Edgar McCarvill, 14 July 2012 19:59

Powered oscillator using ignitron switches

P. D. Nonn, A. P. Blair, K. J. McCollam, J. S. Sarff, and D. R. Stone

Department of Physics, University of Wisconsin-Madison, Madison, Wisconsin 53706, USA

(Received 28 December 2010; accepted 15 April 2011; published online 3 June 2011)

A 10-MVA-scale resonant oscillator, powered by a pulse-forming network and switched with a pair of commutating mercury ignitrons, was developed for the MST reversed-field pinch plasma-confinement experiment. A novel feature of this circuit is its commutation mechanism, wherein each turning on of one ignitron causes a reverse voltage transient that turns off the other. Two of these oscillators are used in oscillating-field current-drive tests, in which they are capable of nearly 1MW net input power to the plasma, with resonant frequencies of a few 100 Hz for pulse durations of a few tens of ms, being precharged for immediate full amplitude. We describe the circuit and its operation, and discuss features that allow reliable, high-current commutation of the ignitrons and exploit their low switching impedance. © 2011 American Institute of Physics. [doi:10.1063/1.3589266]

I. INTRODUCTION

With the capabilities of high hold-off voltage (~ 50 kV), fast turn-on time (< 1 μ s), high current (~ 100 kA), and a small forward drop when conducting (~ 20 V), mercury ignitrons¹ have long served experimental plasma physics as high-power, single-pulse switches. Their tendency, at the end of life or upon abuse, for gradual rather than catastrophic failure distinguishes them from hot-cathode and solid-state switches. They can also be efficient, high-power oscillator switches, if they can be turned off frequently enough. Typically, an ignitron conducts until its forward current is reduced to a few A and its internal arc is extinguished; then, after a few ms it can once more hold off high voltage. However, it can be turned off by a brief (< 0.1 μ s) pulse of reverse current, comparable in magnitude to the current it carried forward, such that the reverse voltage clears the charge carriers from its anode-cathode space. Bronner² reported turning off ignitrons carrying ~ 100 A in single shots by momentarily reversing conducted current for a few μ s.

In this paper, we report on our application of this idea, which is an LC oscillator synchronously switched by a pair of commutating ignitrons and so used to drive a sustained oscillation in a plasma-circuit load. It is powered by a pulse-forming network (PFN) and precharged for immediate full amplitude of up to 10 kV. In each commutation the turning on of one of the ignitrons in the pair produces a reverse voltage transient sent to turn off the other. To our knowledge this is the first such use of ignitrons for this purpose. Two of the oscillators, each capable of tens of MVA reactive power, are operated simultaneously on the MST reversed-field pinch plasma-confinement experiment³ for tests of oscillating-field current drive.⁴⁻⁶ These circuits have allowed such experiments to go forward before the planned implementation of a more comprehensive, expensive system using solid-state high-power switches. Typical PFN-pulse durations are about 25 ms, and the resonant oscillation frequencies have ranged from 200 to 500 Hz, dictated by physics requirements and adjusted by the choice of L and C for the different experiments. This requires repetitive, fast ignitron commutation, switching from kA-level conduction to several-kV hold-off every few ms.

Section II describes the concept, general layout, and basic, measured waveforms during the operation of the circuit. Section III details several special design features added to make it work as intended. Section IV shows its application to the MST experiment with sample measurements of circuit operation during a plasma experiment, and Sec. V is a conclusion with a brief discussion and summary.

II. BASIC CIRCUIT

A basic conceptual schematic of the oscillator is shown in Fig. 1. A resonating LC circuit, or “tank circuit,” drives an oscillation in an inductively coupled load Z . If there is finite resistance in the load or the oscillator itself, then the tank circuit must be supplied by an external source to sustain the oscillation. In our case the external source is a PFN whose output feeds the center tap, or midpoint, of the oscillator’s main inductive coil L , which is composed of the series coils L_1 and L_2 in the figure. This PFN behaves approximately as a current source, and commutation of the two ignitron switches S_1 and S_2 , one periodically connecting one side of the main tank-circuit capacitor C to the ground of the PFN as the other disconnects, allows a portion of the PFN output energy to be deposited into C , replacing the resistive losses and sustaining the oscillation. This oscillation is coupled to Z via the output coils shown above L_1 and L_2 in the figure. The timing of the commutation is ideally such that PFN current flowing through C always charges it with the same as its instantaneous polarity, positive for one half-cycle and negative for the next. This is a class-B oscillator,⁷ in which each of the two ignitron switches is either on for a half-cycle or completely off, and is conventionally called a push-pull oscillator.

Current (I) and voltage ($\propto dI/dt$) waveforms measured with Rogowski coils on our version of this circuit during operation, shown in Fig. 2 during a single cycle, detail how the oscillation is sustained. At the beginning of the cycle pictured, the ignitron S_1 is switched on so that it carries the output current $I_{\text{PFN}} \approx 1$ kA from the PFN, and this disconnects the other ignitron S_2 through the commutation process described later (Sec. III A). This allows a portion of I_{PFN} to flow through C

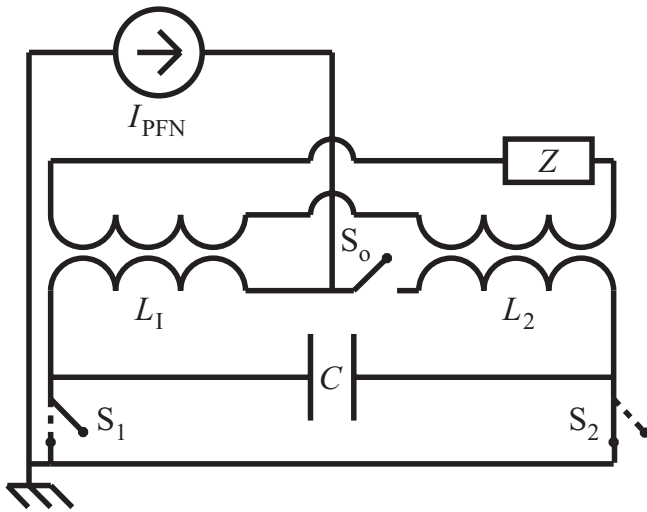


FIG. 1. Conceptual schematic of the driven oscillator with inductively coupled load Z . The ignitron switch S_1 is closed when ignitron S_2 is open and vice versa. Their ideal phasing is such that current from the PFN through the capacitor C always charges it with the same as its instantaneous polarity, sustaining the LC oscillation despite resistive losses in Z or the tank circuit itself. Note that C is first precharged to the PFN voltage so that the oscillation immediately has full amplitude when the switch S_0 is closed to start the pulse.

charging it more positive. As C reaches its maximum positive voltage $V \approx 5$ kV, the tank currents reverse, which begins to discharge C . When V , measured with an unintegrated Rogowski coil signal, crosses a chosen reference voltage V_{ref} from above, which happens just before the maximum negative tank current of around 8 kA, a trigger is sent to turn S_2 on, commutating S_1 off. Here a small discontinuity is evident in dV/dt , after the transient switching noise, corresponding to the jump in I_C and evidencing the driving character of the PFN current. Now the portion of I_{PFN} flowing through C acts

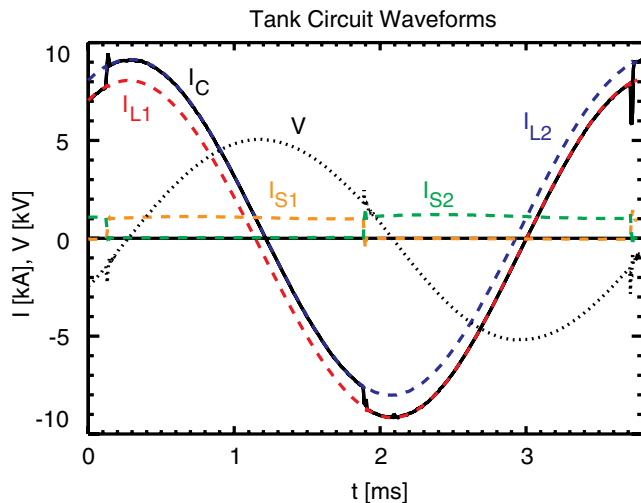


FIG. 2. (Color online) Tank-circuit current (I) and voltage ($\propto dI/dt$) waveforms measured with Rogowski coils during a single cycle of sustained oscillation. In terms of the circuit schematic shown nearby in Fig. 1, the currents through the capacitor (I_C , black solid), the left (I_{L1} , red dashed) and right (I_{L2} , blue dashed) coils, and the left (I_{S1} , orange dashed) and right (I_{S2} , green dashed) ignitron switches are plotted with positive for clockwise tank current in the cases of I_C , I_{L1} , and I_{L2} and positive for anode-to-cathode current in the cases of I_{S1} and I_{S2} , and the voltage across the tank circuit (V , black dotted) is plotted with positive for the right capacitor plate with respect to left.

to charge it more negative. The voltage V reaches its negative peak and then eventually crosses $-V_{\text{ref}}$ from below, which triggers S_1 on and S_2 off, beginning the cycle again. Thus the oscillation in the tank circuit is sustained and is coupled to Z via the output coils (whose current was not measured for this test).

Note that the currents through the two halves of the coil, I_{L1} and I_{L2} , satisfy $I_{L2} - I_{L1} = I_{\text{PFN}} = I_{S1} + I_{S2}$. During this driven oscillation, the actual relative fractions of I_{PFN} flowing through L_1 and L_2 are indeterminate. However, numerical simulations of this circuit (e.g., SPICE) in which the PFN drive of a decaying oscillation is triggered at arbitrary times during the cycle indicate that I_{PFN} initially divides equally, one half flowing counterclockwise through I_{L1} and the other clockwise through I_{L2} . Likewise if in the simulation the PFN is disconnected from the driven tank circuit at an arbitrary time, the now equal tank currents I_{L1} and I_{L2} obtain the average of the values they had just before the disconnection. Measurements of circuit performance and the simulations show that altering the ideal switch phasing described above decreases the drive efficiency for this class-B oscillator. More specifically, the ideal would be $V_{\text{ref}} = 0$ V, whereas we choose V_{ref} to be finite for reliably commutating the ignitrons as described next.

III. SPECIFIC DESIGN FEATURES

Our circuits have several specific design features found either helpful or necessary for reliable operation in experiments. These are addressed here in four subsections: Sec. III A for the commutating ignitrons, Sec. III B for the connection ignitron, which connects the PFN output to the tank circuit, Sec. III C for the PFN itself, and Sec. III D for the air-core transformer coupling the tank circuit to the plasma-circuit load. For reference throughout, a complete oscillator circuit with labels is shown in Fig. 3. The main sequence for a pulse begins with the precharging of both the PFN and tank circuit capacitor C . The pulse, therefore, starts with full oscillation amplitude when the connection ignitron (S_0 in the figure) is triggered, and then the PFN (drawn at the upper left) begins to put current into the tank circuit as the commutation ignitrons (S_1 and S_2) switch back and forth until the PFN charge is depleted. The tank circuit has typical values of $C \approx 1$ mF, a total tank coil inductance of $L \sim 350$ μH (composed of series coils labeled L_1 and L_2 in the figure), and output coil inductance of order 50 μH (composed of L_3 and L_4). The resonant tank frequency, which for no loading would be $1/(2\pi\sqrt{LC})$, is around 250 Hz to meet the physics requirements in this case.

A. Commutating ignitrons

The most important feature of the oscillator circuit is the commutation of the ignitrons used to switch the input current from the PFN. Ignitrons' unique properties not encountered in one-shot switching have required several innovations, which are detailed here.

The commutation system works by feedback to the tank voltage ($\propto dI/dt$), which is sampled inductively by a pair

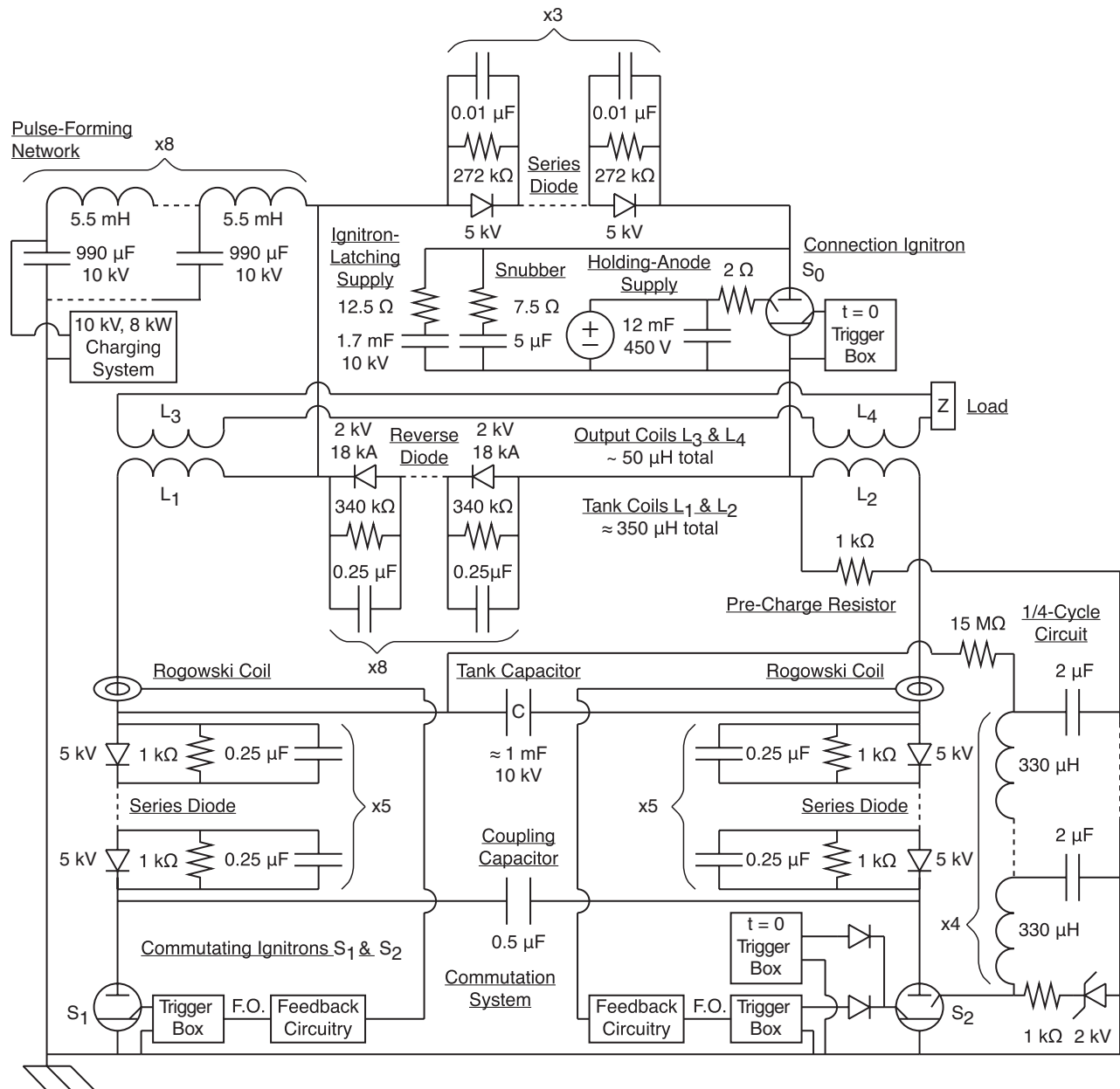


FIG. 3. Detailed schematic of the driven oscillator with MST load.

of Rogowski coils with opposite senses, one leading to each of the commutating ignitrons S_1 and S_2 as shown in Fig. 3. For each of these, the Rogowski signal is low-pass filtered at 1 kHz and input to a falling-voltage comparator, which compares it to a preset V_{ref} . When the filtered Rogowski signal reaches V_{ref} from above, the comparator circuit outputs a fiber-optic signal to an ignitron trigger box, which then sends a trigger pulse having a few- μ s width and a few-kV amplitude to the commutating ignitron igniter, causing that ignitron to connect its anode to cathode. Since this occurs when there is some positive tank voltage on its anode, at the moment the ignitron begins to conduct, the rapid drop in its anode voltage down to ~ 20 V is transmitted as a negative spike via a coupling capacitor of ~ 0.5 μ F to the anode of the other commutating ignitron, which has been conducting. This transient, negative voltage spike on its anode turns it off,

if the impulse is enough to sweep the charge carriers from its anode-cathode space. Empirically, at least 1 kV on the anode of the ignitron being turned on seems to be needed in our circuit, and a higher V_{ref} leads to more reliable commutation (but lower driving efficiency). The transient is estimated to be very brief, lasting less than 0.1 μ s. Later, after one half period of oscillation, this commutation process is repeated in the opposite sense as regulated by the feedback system.

The process does not work without diodes in series with the anodes of the commutating ignitrons. These prevent reverse conduction in the ignitron being turned off, which otherwise would lead to a monstrous current surge ($\gtrsim 100$ kA) in the low-impedance S_1 -C- S_2 -ground loop, followed by the rapid L/R decay of all magnetic energy in the coils, a condition abusive even to ignitrons. Also, the series diode serendipitously retains positive anode voltage on the ignitron about

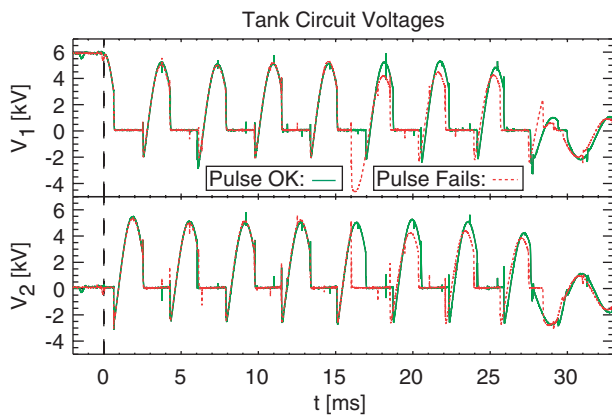


FIG. 4. (Color online) Time dependences of the voltages V_1 (top) and V_2 (bottom) measured with resistive dividers across the series diodes and commutating ignitrons for S_1 and S_2 , respectively, for a pulse with successful commutation (green solid) and a pulse during which one of the ignitrons spontaneously prefires (red dotted). Each pulse is triggered at $t = 0$ (vertical dashed), and the PFN is depleted by $t = 30$ ms.

to be turned on at a level well above the instantaneous tank-circuit voltage on that side, which increases the strength of the commutating transient then coupled to the anode of the other ignitron when it is to be turned off. For this ~ 10 kV oscillator, empirically we found a back-bias rating of ~ 25 kV needed to preserve the life of the diodes, which for us necessitates a diode string with equalizing resistors and capacitors. The resistors do allow some of the tank voltage to drain off the anodes, and just a single diode with no parallel resistance would be ideal.

The commutation process is exemplified in Fig. 4 which shows measurements of two test bursts, one with all proper commutations and one during which a commutation happens to fail. These are measurements of the voltages across the series diodes and commutating ignitrons for S_1 and S_2 taken with resistive dividers, called V_1 and V_2 , with the voltage across the tank circuit being their difference $V_2 - V_1$. When an ignitron is triggered on by the feedback system, the voltage across it and the diode abruptly drops from a few kV to nearly zero as its transmitted impulse turns the other off, causing that voltage to become essentially the tank-circuit voltage, negative for a few $100 \mu\text{s}$ until zero-crossing, after which it swings positive again. Note this measured negative excursion is not really that which turns off the ignitron. That, much more rapid, $\sim 0.1 \mu\text{s}$ transient occurs on the anode itself and is not measured accurately by our diagnostics due to their finite inductance; our voltage measurements across only the ignitrons themselves, digitized at a few MHz sampling rate, read nearly zero from the moment of triggering until the tank-circuit zero-crossing, after which the anode voltage becomes the same as that above the diode as in Fig. 4.

The example of commutation failure in Fig. 4 was not caused by feedback triggering of the ignitron, but instead the ignitron pre-fired spontaneously and spuriously commutated the other ignitron off, despite the design features described in this subsection. As is evident in the figure, pre-firing significantly degrades the oscillation amplitude and perturbs the phase of the oscillator output. This failure mode is the

most common that remains in typical operation, but can be mitigated by choice of ignitron specimens. We have found that an igniter resistance above about 100Ω tends to be needed for good performance and some specimens seem to perform better after several conditioning pulses. Typical minimum failure rates are around 10% of PFN pulses. One might expect, keeping both the tank voltage amplitude and V_{ref} the same, that higher operating frequencies make commutation more challenging in that an ignitron just commutated off will have less time before which it must hold off a particular voltage. A previous version of this system ran at ~ 500 Hz rather than the present ~ 250 Hz and was not as reliable, but then the circuit was still being developed.

The comparator circuit has time-filtering, trigger hold-off functionality so that spurious signals into the comparator do not cause unwanted ignitron triggering. After each nominally legitimate trigger the comparator circuit is disabled for a bit less than one oscillation period, and each ignitron's feedback circuitry also has an initial hold-off appropriate to its correct time of first firing. In terms of Fig. 3, ignitron S_1 is triggered on after the first quarter cycle and S_2 after the first three quarters, as shown in Fig. 4. Note that our previous designs used unfiltered signals from resistive voltage dividers sampling the tank voltage rather than filtered Rogowskis and this resulted in enough high-frequency noise on the comparator inputs to cause false triggers that prevented reliable operation.

The cathodes of all three ignitrons in the oscillator circuit, i.e., the two commutating ignitrons and the connection ignitron (Sec. III B) are cooled with air from the cold output of a vortex tube fed with compressed air. Such cooling is known to benefit the voltage hold-off capability of an ignitron by lowering the mercury vapor pressure inside it and by encouraging recondensation onto the cold cathode rather than hot anode. We think it may also make commutation more reliable, although we have not systematically confirmed this. All the ignitrons in our system are size-D. Previously we used size-A for S_1 and S_2 , but the D-sized work just as well and have a larger Coulomb limit of around 100 C, which is a measure of how much total throughput charge per pulse they can tolerate over the long term.

A small, auxiliary PFN for S_2 called the quarter-cycle circuit is also shown in Fig. 3. Its main job is to make S_2 conduct immediately at $t = 0$, reducing the startup voltage transient from the anode of S_1 to ground, which otherwise would reach about twice the PFN charge voltage during the first quarter-cycle. The circuit is precharged along with the tank circuit (Sec. III C) to a Zener-limited 2 kV, with its output tied to S_2 's holding anode. Meanwhile there is an extra ignitron trigger box that fires the igniter of S_2 at $t = 0$. Thus, although there is zero voltage on the anode of S_2 just before $t = 0$, this trigger along with the quarter-cycle circuit's PFN output turns S_2 on at a phase in which it would be on during fully developed oscillation. This PFN has a pulsewidth of about $200 \mu\text{s}$, long enough to develop ignitron conduction as the main PFN fires, but short enough that it does not interfere with commutation of this ignitron off after the first quarter-cycle. This operation should also slightly increase the overall driving efficiency.

B. Connection ignitron

The connection ignitron, labeled S_0 in Fig. 3, is used in connecting the PFN output to the center tap of the tank coil at $t = 0$ and to carry tank current on odd half-cycles. Being an ignitron it is unidirectional (at low frequency), so a reverse diode stack, antiparallel to it, carries the tank current on even half-cycles. During that time, since the tank current is much larger than the PFN output current, this diode stack's total forward drop can reverse-bias the ignitron and turn it off; so another diode in series with the ignitron isolates this.

Additional measures have been found necessary to ensure S_0 stays conducting during odd half-cycles. The first is an ignitron-latching supply, which is an RC bank across the anode to cathode. This supply is precharged (Sec. III C) to the tank circuit's voltage and starting at $t = 0$ provides a decaying current through the ignitron of at least 100 A for the entire duration of the PFN pulse. The second is a holding-anode supply, which is a ~ 12 mF capacitor in series with a $\sim 2 \Omega$ resistor charged before the pulse by a rectified source to around 400 V and which provides about 200 A through the ignitron's holding anode during the PFN pulse.

It is unclear why both of these measures are needed, but possibly reciprocal voltage transients from the nonlinear plasma load are responsible for otherwise turning off S_0 . This ignitron still sometimes turns off unexpectedly, nearly always during the even half-cycles, when it is not conducting tank current. If a tank current of over ~ 100 A in S_0 were to suddenly cease late in an odd half-cycle, the resulting inductive voltage surge would reverse-bias the reverse diode stack to destruction. To prevent this outcome a $5 \mu\text{F}$ snubbing capacitor holds such an inductive spike below about 5 kV, should S_0 open below 800 A. Note that previous versions of our circuit used a 2 kHz burst of triggers to the igniter of S_0 to maintain conduction whatever its anode voltage was doing. In combination with the holding-anode supply this was effective, but tended to result in unwanted phase perturbations on the oscillating output, as the timing of the discrete bursts did not always match the zero-crossings of the tank current. This motivated replacing it with the ignitron-latching supply.

C. Pulse-forming network

This oscillator circuit has a quality factor Q of around 10 that does not depend much on the loading. Therefore, precharging of the tank circuit is used to get immediate full amplitude at $t = 0$; otherwise it would take a few cycles for the PFN to drive the oscillation up to full amplitude. As seen in Fig. 3, the ~ 1 k Ω resistor on the L_2 side allows the tank circuit C to be precharged to the PFN voltage before each pulse from the same source, a commercial 10 kV, 8 kJ/s capacitor-charging supply.

The PFN for each oscillator contains $n = 8$ series sections of $L_{\text{PFN}} = 5.5$ mH and $C_{\text{PFN}} = 3 \times 330 \mu\text{F} \approx 1$ mF for an output pulse of $2n\sqrt{L_{\text{PFN}}C_{\text{PFN}}} \approx 40$ ms in maximum duration,⁸ and these can be jumpered into different configurations to better match the tank circuit load or to change the pulselength. The PFN coils are the Brooks type which maximizes the inductance per length of wire,⁹ which is $2/0$

building cable. A basic goal in tuning the PFN and tank circuit is a flat voltage envelope for the sustained tank-circuit oscillation, which occurs if the net PFN power delivered into the tank circuit matches its resistive power losses. Part of the losses come from series resistance R_{tank} in the tank circuit itself and part from resistance R_{load} in the plasma-circuit load. Neglecting PFN resistance, if R_{tank} dominates then the matching condition is roughly that the PFN impedance $Z_{\text{PFN}} \sim \sqrt{L_{\text{PFN}}/C_{\text{PFN}}} \approx 2.5 \Omega$ should be about equal to $L_{\text{tank}}/(C_{\text{tank}}R_{\text{tank}}) \approx Q\sqrt{L_{\text{tank}}/C_{\text{tank}}}$, which is the approximately the case for our system. If instead R_{load} were to dominate, then the condition above would be $\sqrt{L_{\text{PFN}}/C_{\text{PFN}}} \sim R_{\text{load}}$. In any case, if Z_{PFN} is too large the oscillation envelope will ramp down since I_{PFN} is too small, and vice versa.

D. Air-core transformer

Each oscillator is coupled to a transmission line leading to its plasma-circuit load by an air-core transformer. Both primary (tank) and secondary (output) coils are composed of pancake-type sub-coils coaxially interleaved to maximize coupling, and these are typically wound with either four (for the primary) or two (for secondary) rows of order ten turns each of $4/0$ welding cable. There are two key differences between an air-core and a typical iron-core transformer in this context: first, the self-inductances of the primary and secondary coils are not very large compared to other inductances in the whole system, and second, the leakage inductances are not negligible compared to the self-inductances. Leakage inductance is defined as the self-inductance of a coil with the coil on the other side of the transformer shorted. Some leakage inductance can be helpful by decreasing the stiffness of coupling which, for the oscillator loaded by a nonlinear plasma, improves the regularity of the resonant frequency and amplitude, at the cost of some drive efficiency.

The ratio L_p/M is equivalent to a turns ratio of primary to secondary quoted for an iron-core transformer and is similar to the actual ratio of turns in the air-core transformer. Here L_p is the primary coil self-inductance and M is the mutual inductance between primary and secondary, which is available from the formula $M^2 = L_p(L_s - L_{sl})$, with L_s the self-inductance and L_{sl} the leakage inductance of the secondary coil. Finally, L_{sl} appears in series with any other inductances on the secondary side of the system, all multiplied by $(L_p/M)^2$ and taken parallel to L_p , in the equivalent circuit, an example of which is shown in Sec. IV.

IV. APPLICATION TO THE MST EXPERIMENT

With the refinements detailed above, the oscillators work reliably at 2 MW RMS output into resistive test loads, but their real application is the mostly inductive loads on the MST plasma-confinement device, which is the focus of this section. The two oscillators generate sinusoidal loop voltages around the MST plasma in the poloidal and toroidal directions, respectively, for tests of oscillating-field current drive (OFCD).⁴⁻⁶ Each oscillator is coupled inductively to its MST load. The toroidal-loop voltage oscillator, called the BP for the poloidal magnetic field it modulates,

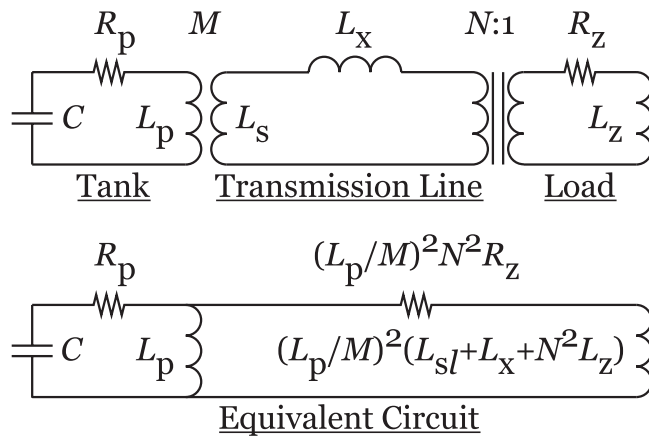


FIG. 5. Schematic of an oscillator inductively coupled to its MST load through a transmission line (top) and an equivalent circuit (bottom). The tank circuit values are C , R_p , and L_p , and M is the mutual inductance between L_p and the output coil L_s , which form an air-core transformer. The transmission line inductance is L_x . At the end of the transmission line is an iron-core transformer with turns ratio $N:1$ and practically infinite magnetizing inductance. The plasma-circuit load values are R_z and L_z . The equivalent circuit load involves the leakage inductance $L_{sl} = L_s - M^2/L_p$.

couples to the plasma in the MST confinement region through which toroidal current flows. The poloidal-loop voltage oscillator, called the BT for toroidal magnetic field, couples to the aluminum shell of MST through which poloidal current flows, coupling to the plasma (see Ref. 3). In each case there is an iron-core transformer coupling the plasma-circuit load to a transmission line itself coupled via the air-core transformer to the oscillator-circuit source. A schematic of one such configuration is shown in Fig. 5. Other MST circuitry on the transmission lines is not materially involved in the oscillations and is not represented in the figure.

Also shown in the figure is an equivalent circuit for this system, which is helpful in analyzing impedance matching and circuit behavior. For each section of the circuit, justifiably neglecting the series resistance compared to the reactive impedance at the resonant angular frequency allows that frequency to be calculated easily as $\omega = 1/(\sqrt{L_e C})$, where L_e is the parallel combination of the two inductances in the equivalent circuit in Fig. 5. The complicated equivalent load inductance in parallel with the tank circuit self-inductance L_p is $(L_p/M)^2(L_{sl} + L_x + N^2L_z)$, where M is the mutual inductance between the air-core inductances L_p and L_s , L_{sl} is the leakage inductance, L_x is the transmission line inductance, N is the number of turns on the primary side of the iron-core transformer to the (single-turn) plasma circuit, and L_z is the plasma-circuit inductance. The tank circuit and plasma circuit have series resistances R_p and R_z , respectively, while the transmission line resistance is neglected. For both the MST BP and BT oscillator systems, typical circuit values from Fig. 5 are listed in Table I.

While the estimated load resistance is within about one order of the tank series resistance, bigger in one case and smaller in the other, the load inductance is much bigger than the tank inductance in either case. This implies that in single-circuit operation most of the lost power goes into the series tank resistance R_p . The value for $R_p \sim 50$ m Ω

TABLE I. Typical MST circuit values for the BP and BT oscillator systems. The measured or estimated quantities from Fig. 5 are listed with precisions of one or two significant digits. Note (*) the values of C are adjusted by a few percent to tune the two resonant frequencies to match for plasma experiments.

Quantity	BP	BT
C [mF]	1*	1*
R_p [m Ω]	50	50
L_p [μ H]	330	380
$\sqrt{L_p/C}$ [m Ω]	600	600
M [μ H]	120	75
L_p/M	2.8	5
L_s [μ H]	100	40
L_{sl} [μ H]	60	25
L_x [μ H]	20	20
N	20	20
R_z [μ Ω]	100	0.5
L_z [μ H]	3	0.1
$(L_p/M)^2(L_{sl} + L_x + N^2L_z)$ [mH]	10	2
$(L_p/M)^2N^2R_z$ [m Ω]	300	5

estimated from observations of the circuit Q is roughly consistent with the ~ 20 V drop per ignitron and the diode drops for the ~ 1 kA PFN supply current. At the resonant frequency ~ 250 Hz, the reactive impedance of the plasma load is much larger than its resistance, which means not much net power is put into the plasma by each single oscillator compared to the reactive power.

However, the plasma provides a dynamic, nonlinear coupling between the two directions of magnetic field, and the BP and BT oscillators can put significant amounts of net power into the plasma when operating at the same time, as they do in OFCD experiments. Essentially one oscillator couples through the plasma to the other load and changes the phase between I and V in a way that depends on the phase between the two circuits. Example of waveforms from one such pulse are shown in Fig. 6, where OFCD is added to the plasma sustained by the background toroidal induction. Currents measured with Rogowskis and voltages measured with flux loops on the plasma circuits are plotted for both BP and BT starting shortly before the OFCD pulse is applied. The phasing between the respective currents and voltages clearly shows these loads are mostly inductive, and the reactive power involved is a few tens of MVA, much larger than the net OFCD input power of about 200 kW measured for this pulse, which was a test of the plasma current drive by OFCD. Note the plasma current ramps up as a result of OFCD in this case. The oscillators were each operating at ~ 5 kV and tuned to have matching resonant frequencies. The loop voltage V_{tor} on the BP is relatively clean compared to V_{pol} on the BT, which has many discrete spikes indicating magnetic activity and showing that the plasma circuit in this case is not a passive load but a dynamic impedance generating power flows itself.

Other OFCD tests with different phasing between BP and BT have shown net OFCD input powers of ~ 800 kW. We think our system is capable of routine operation at ~ 1 MW net OFCD input, but to date the large modulations at such power levels for a plasma of this temperature have tended to degrade the plasma current rather than increase it.

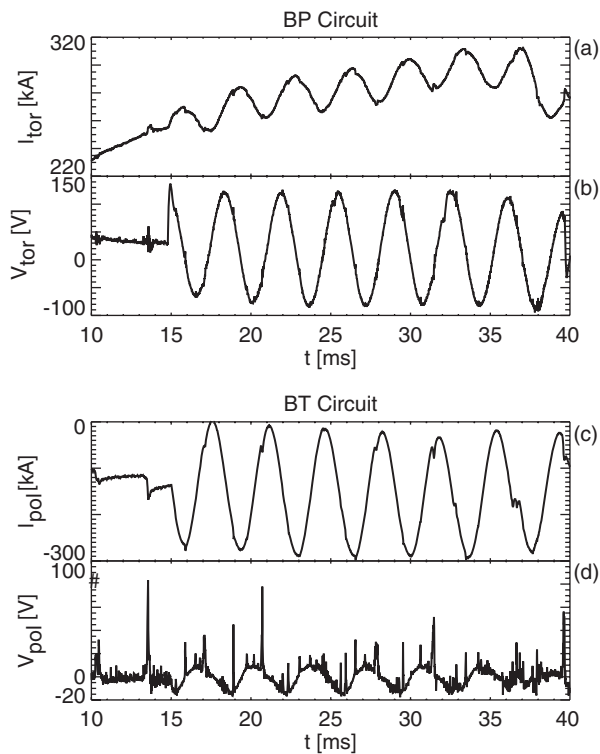


FIG. 6. Data from an MST pulse with both oscillators in operation at once, with currents measured by Rogowski coils and voltages by flux loops. The toroidal current I_{tor} in the plasma (a) and corresponding loop voltage V_{tor} (b) for the BP circuit is shown at the top and the poloidal current I_{pol} in the shell surrounding the plasma (c) and corresponding loop voltage V_{pol} (d) for the BT circuit is shown at the bottom, from a time shortly before the oscillators are triggered until roughly the end of the PFN pulses.

V. CONCLUSION

The ignitron oscillators described above provide a reliable, powerful, and inexpensive way to modulate plasma currents for tests of OFCD and similar techniques, as well as studies of electromotive and fluctuation effects in magnetized plasmas. As implied the key requirement is good commutation performance, and the present design is well optimized to serve the purpose, with one important drawback. To maintain the needed constant phase relationship between the BP and BT we rely on frequency stability with preset trigger times, and despite the somewhat light loading characteristics of our system have found that different background plasma currents and different oscillator power levels both tend to disturb the balance obtained at a particular set of conditions, complicating the research program with circuit retuning. Still, experience with the system has been helpful in teaching us how to use it more effectively, and it is apparently the case that the hard limits on its experimental performance are set by other MST parameters rather than the tank circuits themselves.

If needed, a longer system pulselength would mainly be a matter of lengthening the PFN while providing for the ignitron Coulomb limits to remain satisfied. Our present circuit using size-D ignitrons operates in the neighborhood of their Coulomb limits; the larger size-E, which tend to have limits a few times higher than size-D, might be needed with a longer pulselength. Also, we speculate that the system's

resonant frequency could be increased to around the kHz level with adequate commutation reliability, perhaps with a requisite cost to the driving efficiency. Note that increasing the frequency for the same commutation phasing might degrade reliability by increasing the hold-off requirements on the commutating ignitrons (see Sec. III A), while increasing the commutation threshold V_{ref} to mitigate this would decrease driving efficiency.

Presently, a new programmable power supply for the MST BT system is being commissioned, and one for the BP system is in design. It is planned for these more flexible, more expensive supplies to eventually replace the ignitron oscillators entirely on MST, although in the interim the two systems will be used together, the BT with the programmable supply and the BP with the ignitron circuit. We think the new programmable supplies will allow much better phase control but not that they will be capable of much higher power levels than the ignitron oscillators.

In summary, we have reported on our development and application of 10-MVA-scale, precharged, PFN-driven tank circuits switched by rapidly commutated ignitrons for plasma experiments on the MST reversed-field pinch device. Used as a pair for OFCD tests, the two circuits are capable of injecting up to nearly 1 MW net power into the plasma for a few tens of ms and have been operated at resonant frequencies of a few 100 Hz. The basic principles of circuit operation have been reviewed and particular points on its design and use have been discussed.

ACKNOWLEDGMENTS

The oscillator was conceived by Tom Lovell (deceased) over a decade ago. His simulations including his model of ignitrons as commutated switches accurately predicted much of the circuit's behavior, and his suggestions during development helped us simplify and improve the design. We thank Mark Thomas for useful conversations and Jason Kauffold for work on construction, maintenance, and documentation of the hardware.

This work was supported by the US DOE.

¹D. B. Cummings, *Pulsed Power Ignitron Switches*, Tech. Rep. UCRL-88168 (Lawrence Livermore National Laboratory, Livermore CA, 1984).

²G. Bronner, "Turning Off" Gas Discharge Tubes (Ignitrons and Thyrotrons) in D. C. Operation, Tech. Rep. 113 (Atomic Energy Commission, 1960).

³R. N. Dexter, D. W. Kerst, T. W. Lovell, S. C. Prager, and J. C. Spratt, *Fusion Technol.* **19**, 131 (1991).

⁴A. P. Blair, "Oscillating Field Current Drive Experiments in the Madison Symmetric Torus," Ph.D. thesis, University of Wisconsin-Madison, 1150 University Ave, Madison WI 53706 (2006).

⁵K. J. McCollam, A. P. Blair, S. C. Prager, and J. S. Sarff, *Phys. Rev. Lett.* **96**, 035003 (2006).

⁶K. J. McCollam, J. K. Anderson, A. P. Blair, D. Craig, D. J. Den Hartog, F. Ebrahimi, R. O'Connell, J. A. Reusch, J. S. Sarff, H. D. Stephens, D. R. Stone, D. L. Brower, B. H. Deng, and W. X. Ding, *Phys. Plasmas* **17**, 082506 (2010).

⁷L. Gray and R. Graham, *Radio Transmitters* (McGraw-Hill Book Company, Inc., New York, 1961).

⁸G. N. Glasoe and J. V. Lebacqz, *Pulse Generators* (McGraw-Hill Book Company, Inc., New York, 1948).

⁹F. W. Grover, *Inductance Calculations* (D. Van Nostrand Co., New York, 1946).